Ultrafast intramolecular electronic energy transfer in rigidly linked aminopyrenyl–aminobenzanthronyl dyads—a femtosecond study

Miroslav Dvořák,[*a] **Vlastimil Fidler,**[a] **Peter W. Lohse,**[b] **Martin Michl,**[a] **Kawon Oum,**[c] **Philipp Wagener**[b] and **Jörg Schroeder**[bc]

Ultrafast electronic excitation transfer (EET) followed by structural and vibrational relaxation (VER) of the acceptor have been characterised using transient absorption and transient lens techniques.

Introduction

Understanding the dynamics of electronic energy exchange between subunits in complex molecular structures is essential for a successful design of nanoscale photonic devices[1–3] that might also be used to mimic efficient biological antenna systems.[4] It is controlled by electronic coupling that mediates electron and/or excitation energy transfer.[5–9] At the same time, concurrent radiationless processes may enhance or diminish the electronic communication between subunits.[5,6] As it is essential to suppress or at least minimize unwanted processes that might degrade the transfer efficiency, it is important to understand in detail the intramolecular dynamics in bi- or multichromophoric systems. Of interest in this context also is intermolecular vibrational energy relaxation (VER) of excited electronic states that may significantly affect transfer rates, if electronic coupling between participating states is strongly affected by vibrational excitation. Vibrational cooling of electronic excited states causes a characteristic temporal evolution of transient spectra that may be monitored by ultrafast spectroscopy.[7–11]
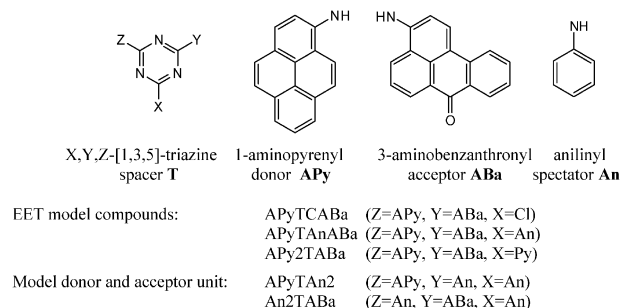
Following the discovery of pyrene excimer formation by Förster and Kasper,[12] pyrenyl groups have played a prominent role as chromophores in covalently linked systems to investigate the dynamics of exciplex formation and electron transfer[13–22] as well as intramolecular electronic excitation energy transfer (EET) in solution.[23–26] Recently, we reported on a donor–acceptor system consisting of a rigid s-triazine ring spacer (T) connecting an aminopyrene type donor unit (APy) and an aminobenzanthrone type acceptor unit (ABa), see Scheme 1.[27] Not unexpectedly for this comparatively rigid structure,[28,29] we found strong evidence that intramolecular EET from the initially excited APy donor to the ABa acceptor is extremely efficient and takes place on a $\sim 10^{-13}$ s time scale.[30,31] The sub-picosecond EET rate suggests that energy transfer is of the through-bond type, as a rough estimate of the rate constant for Förster-type excitation transfer is two orders

of magnitude too small. Furthermore, the transient acceptor fluorescence anisotropy showed a noticeable effect of enhanced donor–acceptor vibronic coupling on EET with increasing excitation energy, suggesting that EET occurs before intramolecular vibrational energy redistribution (IVR) is complete.[31] A still open question is, however, whether the initial excitation populates an electronic state localized on the donor subunit or a delocalized state encompassing both donor and acceptor moiety. In our studies so far we found no clear cut evidence for a local donor precursor state being populated prior to the appearance of acceptor emission.

In this paper we report on femtosecond pump–probe measurements in search for possible evidence for a precursor state and looking in more detail into the issue of vibronic excitation in the class of APyTXABa compounds, X being Cl, APy or An as shown in Scheme 1. In particular, we address the issue of vibrational cooling in the electronically excited state and its possible influence on intramolecular EET as well as the effect of different X-subunits on the triazine ring.

Experimental

Details of the pump–probe set-up for transient absorption measurements have been described elsewhere.[32] In brief, we used a 1 kHz Ti:sapphire regenerative amplifier (Clark-MXR CPA2001) as the femtosecond light source delivering pulses of 0.9 mJ energy and 150 fs duration at 773 nm which were used to pump two commercial optical parametric amplifiers, a Jobin Yvon two stage NOPA (1/3 of pump intensity) and a Light Conversion TOPAS (2/3 of pump intensity). After

[a] *Department of Physical Electronics, Faculty of Nuclear Science and Engineering, Czech Technical University, V Holešovičkách 2, 180 00 Prague 8, Czech Republic. E-mail: dvorakm@fjfi.cvut.cz*
[b] *Institute of Physical Chemistry, University of Göttingen, 37077 Tammannstr. 6, Germany*
[c] *Department of Spectroscopy and Photochemical Kinetics, Max-Planck-Institute of Biophysical Chemistry, 37070 Göttingen, Germany*

X,Y,Z-[1,3,5]-triazine spacer **T**	1-aminopyrenyl donor **APy**	3-aminobenzanthronyl acceptor **ABa**	anilinyl spectator **An**

EET model compounds:	APyTCABa (Z=APy, Y=ABa, X=Cl)
	APyTAnABa (Z=APy, Y=ABa, X=An)
	APy2TABa (Z=APy, Y=ABa, X=Py)
Model donor and acceptor unit:	APyTAn2 (Z=APy, Y=An, X=An)
	An2TABa (Z=An, Y=ABa, X=An)

Scheme 1 Building blocks and compounds investigated in this study.

frequency doubling these provided tunable pump and probe pulses, respectively. The spectral width of the pump pulses at 350 nm was measured to be about 7 nm (assuming Gaussian band shape), corresponding to a pulse duration of ~ 140 fs, their energy was approximately 0.05 μJ. Probe pulses were taken directly from the computer-controlled TOPAS using its internal nonlinear mixing and wavelength separation facilities. Their spectral width was about 5 nm throughout the spectral range 460–760 nm covered in our experiments. We used a conventional pump–probe arrangement employing an optical delay line with nominal 0.7 fs step size. Incident and transmitted probe pulse energies were measured by integrating photodiodes (Hamamatsu 1226-8BQ or 1336-8BQ0A). Pump and probe beams were focused into the 1 mm sample cell by parabolic mirrors to beam waist diameters of approximately 300 μm and 150 μm, respectively, in a non-collinear geometry at an angle of about 7°. Relative polarization of pump and probe beams was controlled by a tunable zero order half-wave plate. Depending on pump and probe wavelength, the pump–probe cross correlation FWHM in this setup varied between 120 and 240 fs. Experiments were performed under magic angle conditions. Transient absorbance traces were taken by recording incident to transmitted probe pulse energy ratios alternating between pump pulse on and off, *i.e.* in synchronization with a chopper positioned in the pump pulse beam. At each delay position, 200 to 1000 measurements were averaged, and every final trace was the result of 4 to 6 scans over the whole time range.

Details of the principle and experimental set-up for the transient lens (TL) measurement can be found in ref. 33. A mode-locked Ti:sapphire laser (Spectra-Physics Tsunami) pumped by a Nd:YVO$_4$ laser (Spectra-Physics Millenia Xs) generated pulses at 740 nm or 800 nm with a repetition rate of 82 MHz and an average power of about 1.5 W. Part of the laser beam was amplitude modulated at 2 MHz by an acousto-optic modulator and subsequently frequency-doubled in a LBO crystal to generate a 370 nm (400 nm) pump beam with pulse energies <0.1 nJ. The remaining part was used as probe beam (pulse energy <1 nJ). The pump–probe cross correlation FWHM in this setup was <120 fs. Pump and probe beams were recombined in a collinear beam-in-beam arrangement, with the polarization set to parallel before passing through a 1 mm sample flow cell which was mounted on a linear translation stage. Dual-beam two-color Z-scans were measured by recording the lens signal of the solution at different distances Z with respect to the focal plane for a specific pump–probe delay time. TL and Z-scan signals were detected by an avalanche photodiode (200 μm active diameter) in the far field and fed into a lock-in amplifier employing the 2 MHz modulation as a reference signal. An appropriate correction procedure described as "convex–concave–lens (CCL) method" in ref. 33 was used to estimate the transient absorption contribution of the solute: The absorption contributions in TL signals were selectively removed by taking the difference in TL measurements performed at two symmetrical prefocal ($-Z$) and postfocal ($+Z$) positions, where the transient absorption signals were identical. The Kerr lens contribution of the solvent was removed by subtracting "solvent-only" pump–probe measurements under the same conditions such that the pure TL signal was obtained.
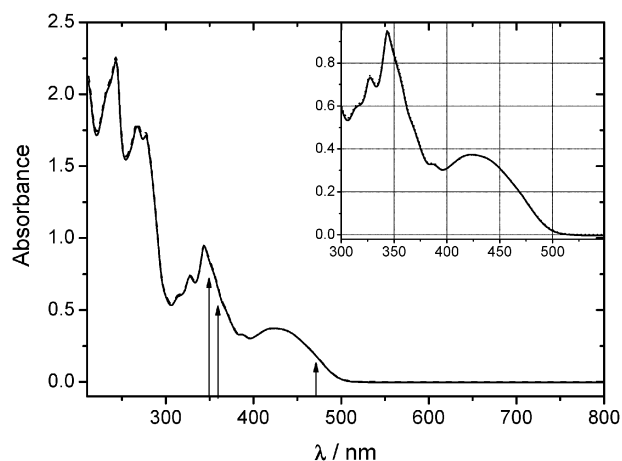

Fig. 1 Stationary absorption spectrum of APyTAnABa in dioxane (concentration $\sim 5 \times 10^{-4}$ M) before (solid line) and after (dashed line) pump–probe run. Arrows indicate excitation wavelengths.

Syntheses and specifications of APyTCABa, APy2TABa, APyTAnABa, APyTAn2 and An2TABa are described elsewhere.[27,30,34] The compounds were dissolved in spectroscopic grade dioxane. The solutions were prepared to have an optical density at the excitation wavelength in the range of about 0.25 to 1 in a cell of 1 mm optical length. Steady state absorption spectra before and after pump–probe measurements were taken to check the stability of the sample.

Results and discussion

In Fig. 1 we show the stationary absorption spectrum of APyTAnABa. To a very good approximation it can be considered as a linear superposition of the absorption spectra of APy donor and ABa acceptor subunits as may be shown by comparison with suitable model donor and acceptor compounds such as APyTAn2 and An2TABa, respectively.[30,31] Acceptor unit absorption is weak and centers around 430 nm. Excitation occurs into the longest wavelength absorption band of the donor subunit at 350 nm where acceptor part absorption is negligible.[30] A comparison of spectra before and after pump–probe runs under typical conditions shows that a minute amount of bichromophoric solute is consumed and that no products are formed that absorb in the relevant wavelength region. This holds true for all compounds used in this study.

Ultrafast intramolecular EET

In Fig. 2 we compare transient absorption spectra at 1 ps time delay in dioxane solution. The model acceptor An2TABa, which is excited at 473 nm, shows a significantly narrower and blue shifted main transient absorption band compared to that of the model donor APyTAn2 excited at 360 nm. The transient absorption of the corresponding bichromophoric compound APyTAnABa obtained after exciting exclusively into the donor subunit absorption band at 350 nm closely resembles that of the model acceptor, indicating that electronic excitation is already localized on the acceptor subunit after 1 ps. This observation also holds for the two other bichromophores investigated in this
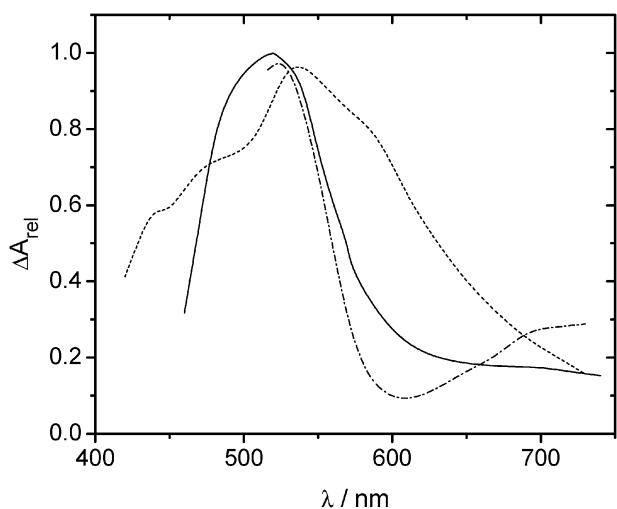
Fig. 2 Transient absorption spectra in dioxane for 1 ps time delay. Model donor APyTAn2 (dashed line), model acceptor An2TABa (dotted–dashed line) following excitation at 360 nm and 473 nm, respectively, and bichromophore APyTAnABa excited at 350 nm (solid line).
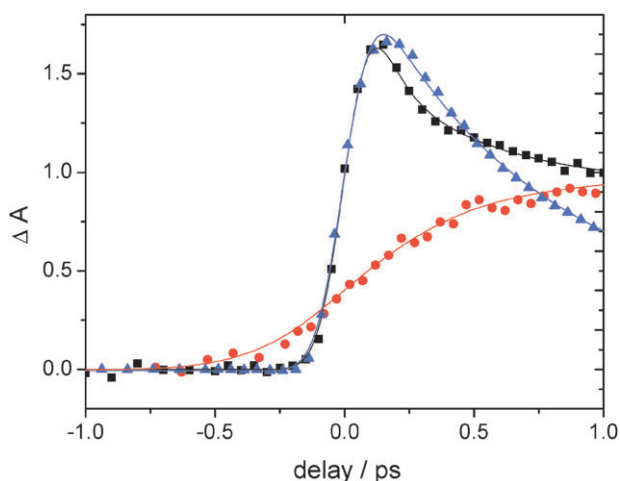

Fig. 3 Transient absorption signals (red and black) of APyTCABa in dioxane probed at 750 nm compared with signal of ABa (blue) pumped at 350 nm and probed at 740 nm in the same solvent. Black squares: excitation at 473 nm into the acceptor absorption band; red circles: excitation at 350 nm into the longest wavelength donor absorption band, blue triangles ABa pumped at 350 nm The solid lines are fits using a convolution of Gaussian pulse shapes with a single exponential. Parameter values are given in the text.

study and is in agreement with our earlier conclusion that EET in these compounds is very rapid.[31]

As there is no donor transient absorption at wavelengths above 750 nm, one can observe acceptor excited state formation directly as an absorption rise in this spectral region. In Fig. 3 we compare the transient absorption rise of APyTCABa in dioxane solution at 750 nm probe wavelength after excitation into the acceptor absorption band at 473 nm with that obtained upon exciting the donor subunit at 350 nm. In the first case, the rise time should be determined by the pump–probe cross correlation of our experimental set-up, while in the second experiment the finite EET transfer rate from donor to

acceptor unit should slow down the absorption rise. This is exactly what we observe: excitation at 473 nm leads to an instantaneous absorption rise corresponding to a pump–probe cross correlation width of $\tau_{cc} = (140 \pm 10)$ fs followed by a 200 fs decay which is of no importance here, while following 350 nm excitation there is a significantly slower absorption rise. This can be compared to a signal obtained with amino-benzanthrone, a compound showing instantaneous transient absorption of the Franck–Condon excited state, at the same pump and probe wavelength and in the same solvent. In this case, the rise is equivalent to the cross-correlation width, which is $\tau_{cc} = (140 \pm 10)$ fs. Taking this value we obtain an upper limit for the single exponential rise time constant of (350 ± 100) fs. Assuming alternatively that the slow rise is caused entirely by a longer cross correlation gives $\tau_{cc} = (590 \pm 50)$ fs, a value which seems to be unrealistically large. These experiments, therefore, lend further support to our previous conclusion[31] that intramolecular EET occurs on a time scale of 100–300 fs.

For the main part of this study, the three bichromophores APyTCABa, APy2TABa, and APyTAnABa dissolved in dioxane were excited into the donor-localized state at a pump wavelength of 350 nm which led to strong acceptor type transient absorption in the spectral region between 460 and 760 nm. Transient absorption traces in dioxane show a characteristic probe wavelength dependence with little variation between the compounds, as illustrated for APyTCABa at different probe wavelengths (Fig. 4 left) and for the three compounds at 500 nm probe (Fig. 4 right).

From such traces, which were recorded at 10 to 20 nm probe wavelength intervals and subsequently fit by a convolution of a Gaussian pulse with a sum of exponential functions, we reconstructed the transient spectra shown in Fig. 5 for selected delay times. The spectra feature a strong band at 510 nm with significant time evolution, and a weak, almost time-independent band at around 710 nm. Within the first 50 ps the main band undergoes a 15 nm blue shift and narrows noticeably, remaining then constant up to the maximum time delay of 200 ps.

To analyze their time evolution in more detail, we fitted two Gaussian peaks centered at 510 and 710 nm to the spectra and subsequently subtracted the constant 710 nm band. Considering that for all three compounds the remaining main peak may be assigned exclusively to acceptor type absorption, we first look at the time dependence of the band integrals, ignoring the temporal evolution of the spectral band shape and position. All three band integrals show an ultrafast almost step-like rise
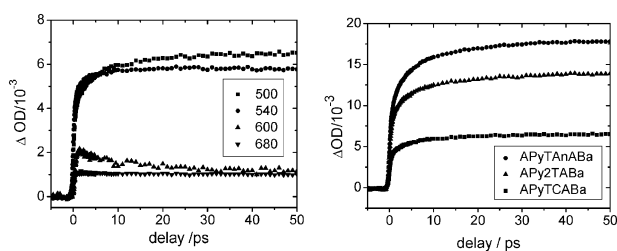

Fig. 4 Transient absorption traces in dioxane following excitation at 350 nm of (left) APyTCABa at selected probe wavelengths, and of (right) the three bichromophores at 500 nm probe wavelength.
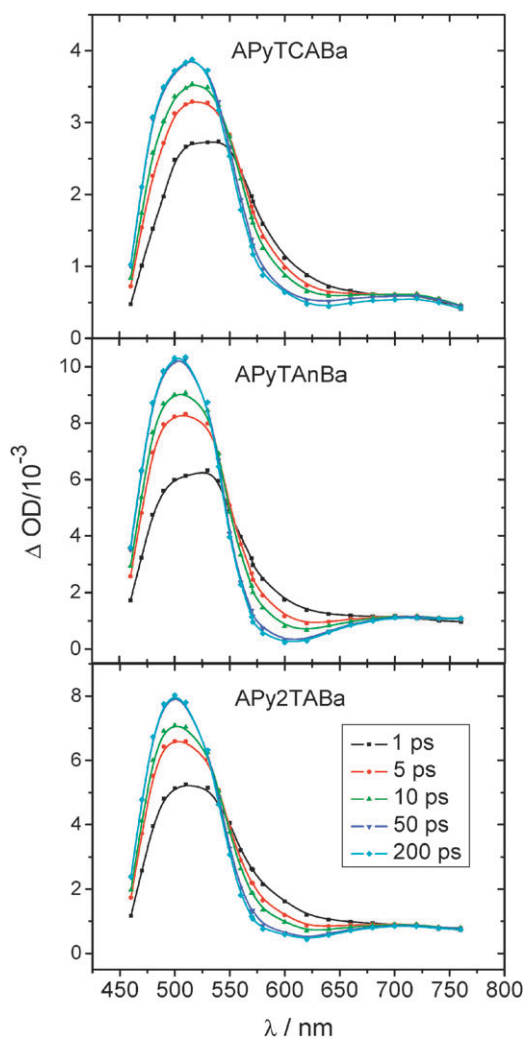
Fig. 5 Reconstructed transient absorption spectra of APyTCABa (top), APyTAnABa (middle) and APy2TABa (bottom) in dioxane at probe pulse delays of 1, 5, 10, 50, and 200 ps. The compounds were pumped in the donor absorption band at 350 nm. The wavelengths at which kinetics were recorded are marked by points.

with a time constant close to the experimental time resolution of ~ 300 fs to about 75% of their final amplitude, followed by a further rise with an average time constant $\tau_{av} \approx 2$ ps (Table 1, Fig. 6). Thus in addition to the main ultrafast EET process, there is evidence for another "slow" contribution. This could be a signature of a slow-down of EET caused by decreasing coupling between donor and acceptor subunits as a consequence of intramolecular vibrational energy redistribution depopulating the initially excited Franck–Condon state. Another possibility would be that EET takes place a to short-lived electronically excited S_x-state of the acceptor moiety
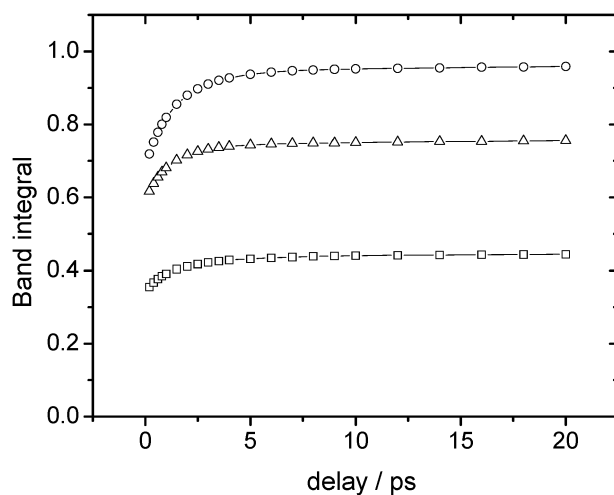

Fig. 6 Time evolution of the main band integral of the three bichromophores in dioxane following excitation at 350 nm. ($\square$): AyTCABa, ($\triangle$): APy2TABa, ($\bigcirc$): APyTAnABa. The initial part of the ultrafast rise below a time delay of 200 fs is not resolved here. Solid lines represent triexponential fits to the data.

which subsequently internally converts on a ps time scale to the local electronic S_1-state of the acceptor. In this case the oscillator strength of the $S_n \leftarrow S_1$ transition would have to be about 30% larger than that of the $S_n \leftarrow S_x$ transition. The S_1-state can be identified with the long-lived fluorescent state observed previously[30,31] Alternatively, both S_1 and a dark S_x-state could be populated by EET with an overall rate coefficient of $\sim 3 \times 10^{12}$ s^{-1} and a branching ratio of 3 : 1 in favour of the S_1-state. Subsequently, one would observe $S_1 \leftarrow S_x$ internal conversion at a rate of ~ 2.5–5×10^{11} s^{-1}. These two possibilities cannot be distinguished on the basis of the transient absorption experiment alone.

Additional insight comes from a comparison of transient lens (TL) signals shown in Fig. 7 that were obtained from APyTCABa at excitation wavelengths 400 nm and 370 nm. Exciting the acceptor moiety at 400 nm results in a net signal increase following the 400/800 nm-pump–probe cross-correlation time of 200 fs to a constant value, indicative of directly populating the acceptor excited state with no ensuing intramolecular electronic dynamics. At 370 nm pump wavelength, exciting predominantly the donor moiety, the signal to noise ratio is much worse. In spite of the high noise level one may observe that (1) the 370/740 nm-pump–probe cross-correlation time is shorter (~ 100 fs), (2) the signal rise is somewhat slower (~ 200–300 fs), and (3) followed by a slight decay on a time scale of 2–4 ps.

The 200–300 fs rise of the TL-signal upon donor excitation is consistent with our current estimate of the time constant for EET to the acceptor, while the ps-decay matches the

Table 1 Time constants τ_i and relative amplitudes A_i of double exponential fits to the evolution of main band integrals

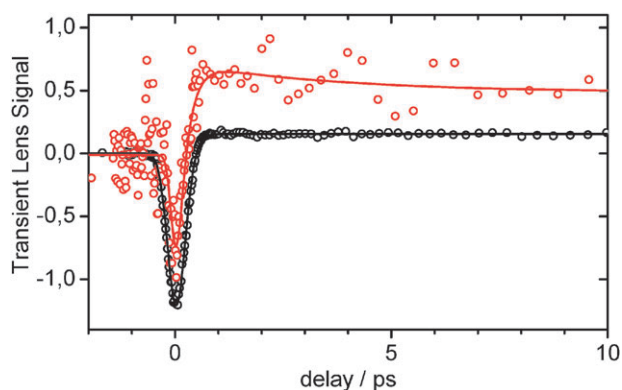|	τ_1/ps	A_1	τ_2/ps	A_2	τ_{av}/ps
APyTCABa	0.9(6)	−0.061	4.0(9)	−0.042	2.2
APy2TABa	1.1(7)	−0.140	7.1(4)	−0.023	2.0
APyTAnABa	1.1(2)	−0.197	3.5(4)	−0.076	1.8

Fig. 7 Transient lens signals of APyTCABa in dioxane (Kerr effect and transient absorption removed, see experimental section) for 400 nm (black) and 370 nm (red) excitation taken at 800 nm and 740 nm, respectively. Open circles are measured data, solid lines optimized fits including convolution with a Gaussian cross-correlation function.

corresponding life time component observed in the absorption band integral rise. It appears, therefore, that this "slow" component has to be associated with changes in the character of the acceptor excited electronic state rather than with a slow-down of donor–acceptor EET caused by IVR decreased donor–acceptor coupling. The latter would show up as a further increase of the TL-signal instead of a decay. It also is consistent with purely sequential dynamics

$$S_1(FC-Donor) \xrightarrow{EET} S_x(Acceptor) \xrightarrow{IC} S_1(Acceptor).$$
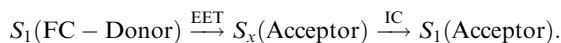
A combined competitive/sequential model of the kind suggested above,

$$S_1(FC-Donor) \xleftarrow{EET(75\%)} S_1(Acceptor)$$
$$\xrightarrow{EET(25\%)} S_x(Acceptor) \xrightarrow{IC} S_1(Acceptor)$$
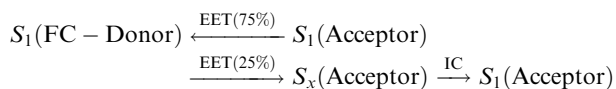
would require that the S_x state possesses a much higher electronic polarizability than the S_1-state in order to be in agreement with the observed decay of the TL signal.

Vibrational relaxation

In order to separate population dynamics from spectral evolution, we normalized the transient spectra to their respective band integral (Fig. 8). The three sets of normalized spectra clearly show the blue shift and band narrowing with increasing time delay. Together with the narrow isosbestic region to the red of the band maximum this indicates that spectral dynamics is strongly affected by VER. Integrating the normalized bands in the wavelength range above and below the isosbestic region and comparing the time evolution of these partial normalized band integrals supports this conclusion (Table 2).

In all three cases time constants and relative amplitudes of rise and decay components of both partial band integrals match perfectly. This correspondence of the time evolution of rising and decreasing band sections is illustrated in Fig. 9. In addition, we observe a decrease of time constants upon substituting the chlorine on the triazene ring by anilinyl or aminopyrenyl.

The larger τ_{2P} time constants clearly are associated with vibrational cooling of the hot acceptor subunit S_1 state that
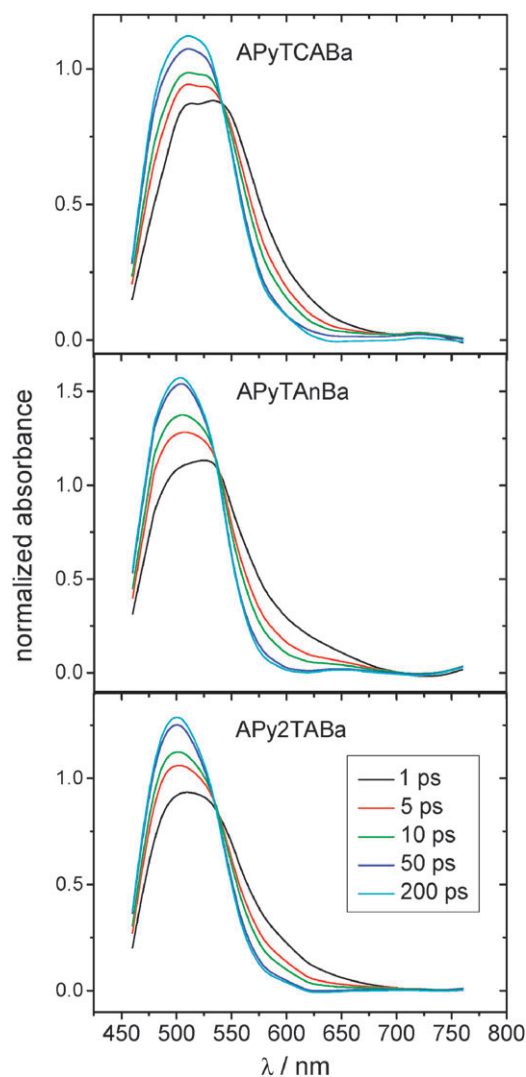

Fig. 8 Band area normalized transient absorption spectra of APyTCABa, APyTAnABa and APy2TABa from Fig. 5. (The weak band at 710 nm was subtracted.)

Table 2 Time constants τ_{iP} and relative amplitudes A_{iP} of double exponential fits to the evolution of partial normalized band integrals in the time range 0–50 ps

	τ_{1P}/ps	A_{1P}	τ_{2P}/ps	A_{2P}
APyTCABa				
Blue center rise	4.1(4)	−0.106	20.0(3)	−0.113
Red wing fall	4.1(4)	0.105	20.0(3)	0.113
APyTAnABa				
Blue center rise	2.5(1)	−0.120	14.7(3)	−0.159
Red wing fall	2.4(1)	0.121	14.7(3)	0.159
APy2TABa				
Blue center rise	1.8(1)	−0.114	13.8(5)	−0.144
Red wing fall	1.8(1)	0.114	13.7(6)	0.144

has been populated by ultrafast energy transfer from an energetically higher precursor state. The slight decrease of τ_{2P} with increasing bulkiness of the third substituent at the triazine spacer unit is consistent with this picture as coupling to the solvent bath is enhanced. The extent to which VER also contributes to the short time constant τ_{1P} is not as obvious. In

This journal is © the Owner Societies 2009

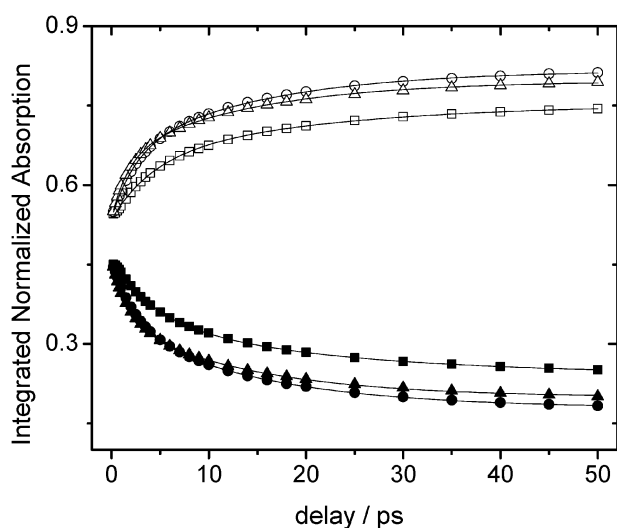*Phys. Chem. Chem. Phys.*, 2009, **11**, 317–323 | 321

Fig. 9 Time evolution of partial band integrals of normalized TA spectra of bichromophores in dioxane. Open symbols: blue center rise; filled symbols: red wing decay. ($\square$,$\blacksquare$): APyTCABa; ($\triangle$,$\blacktriangle$): APyTAnABa; ($\bigcirc$,$\bullet$): APy2TABa.

general, VER of large molecules is characterized by a single time constant that describes the loss of vibrational excess energy to the heat bath.[35] As long as the experimentally measurable quantity is linearly related to this excess energy, a single exponential decay will be observed and the VER time constant can be extracted directly. If the observable is non-linearly dependent on excess energy, a non-exponential decay will result and one needs a calibration to extract the correct VER rate.[36] In our case, the observable is the extinction coefficient $\varepsilon(\lambda)$ for $S_n \leftarrow S_1$- absorption which is not directly proportional to internal energy, and the required calibration is not available. Therefore, the true VER rate constant cannot be extracted from the observed decay. Also, at this stage there is no way to assess the extent to which intramolecular vibrational energy redistribution (IVR) contributes to the early stages of the spectral evolution of the band shape. The band integral and shape analysis implicitly assumes that a single electronic state with constant oscillator strength is responsible for the transient absorption. In the view of the discussion above, however, this assumption is not strictly met, as the evidence suggests that there is a change of electronic state in the acceptor moiety after EET on the time scale of 2–4 ps. The change of band shape observed on this time scale therefore probably also reflects internal conversion to the acceptor S_1-state.

Excited state dynamics

Excited state coupling and delocalization may be susceptible to the degree of vibrational excitation of donor and/or acceptor moiety. Apparently excitation to the Franck–Condon state is accompanied by a large increase of vibronic coupling between the subunits of the bichromophore, such that electronic excitation energy is effectively transferred to the aminobenzanthronyl acceptor part. Competing with EET on the hundred femtosecond time scale is IVR into strongly coupled "dark" vibrational modes. If electronic coupling in these modes was smaller than in the Franck–Condon excited modes, EET as a result would slow down appreciably which could explain the 2–3 ps transient on the absorption band

integral rise. Accepting this picture, however, implies the existence of a donor localized Franck–Condon state for which we found no spectral evidence.

The experimental evidence rather seems to suggest that EET is complete within about 300 fs, *i.e.* that the 2–3 ps transient is indicative of electron density redistribution. This interpretation is also in accord with our earlier fluorescence up-conversion measurements[31] showing a fluorescence anisotropy decay on exactly the same time scale. In principle one would imagine that, *e.g.*, even slight changes of dihedral twist angles between donor, acceptor and spacer groups within a few picoseconds after EET could increase charge localization on the acceptor subunit and in this way enhance acceptor oscillator strength (absorption rise) and decrease overall bichromophore polarizability (TL-signal decay). As a further consequence of charge rearrangement, solvent dielectric relaxation could induce a dynamic spectral shift and transient broadening of the absorption band. As the solvent stabilizes the new charge distribution, absorption intensity could increase on the time scale of solvation dynamics. The time scale of the ~ 2 ps component observed in the integral band intensity rise as well as wing decay and peak rise in the normalized spectra would be compatible the average correlation time $\langle\tau\rangle = 1.7$ ps of the spectral response function measured in dioxane.[37] However, though preliminary results of quantum chemical calculations[38] on APyTCABa indicate that the equilibrium dihedral angle between the aminopyrenyl unit and spacer ring increases from $(19 \pm 4)°$ in the ground state to about $55°$ in the first singlet excited state, so far we found no evidence for substantial local charge rearrangement as a consequence of this twisting motion. Higher level calculations are definitely needed to reach a final conclusion about the proposed interpretation of the observed spectral dynamics.

The overall picture emerging from this pump–probe study on APyTXABa compounds may be summarized as follows:

1. Transient absorption band and TL-signal rise times both indicate that excitation into the donor absorption band at 350–370 nm causes ultrafast intramolecular EET to the acceptor subunit on a time scale of ~ 200 fs. We found no evidence for a local donor precursor state being populated to any measurable extent on this time scale prior to EET. It seems likely, therefore, that excitation directly populates a strongly coupled state that is delocalized across the spacer subunit to the acceptor site.

2. The subsequent 2–3 ps rise of the integral absorption band intensity and simultaneous decay of the TL-signal provide strong indications that ultrafast EET is followed by changes in electronic structure either due to internal conversion to a nearby electronic state or by local charge rearrangement coupled to a rapid structural relaxation.

3. The spectral evolution of the transient absorption band shape suggests that localization of the electronic excitation energy on the acceptor subunit leads to a high degree of vibrational excitation which is transferred to the solvent by VER within 10–20 ps.

Conclusion

Pump–probe absorption and transient lens measurements on the femtosecond time scale on bichromophoric compounds of

the type APyTXABa support earlier reports on ultrafast intramolecular EET upon aminopyrenyl donor subunit excitation. EET is complete on a time scale of about 200 fs, and we found no spectral evidence for a short-lived intermediate precursor state localized on the donor moiety. Excitation is thought to populate a Franck–Condon state delocalized across the triazinyl spacer ring which then relaxes with a time constant of 2–3 ps to a more stable electronic structure. The large amount of initial vibrational excess energy after EET is transferred to the solvent within 10–20 ps.

Acknowledgements

References

1 S. Speiser, *J. Photochem.*, 1983, **22**, 195–211.
2 *Molecular Electronics: Science and Technology*, ed. A. Aviram and M. Ratner, New York Academy of Sciences, New York, 1998.
3 J. M. Tour, *Molecular Electronics: Commercial Insights, Chemistry, Devices, Architecture and Programming*, World Scientific, New Jersey, 2003.
4 D. Gust, T. A. Moore and A. L. Moore, *Acc. Chem. Res.*, 2001, **34**, 40–48.
5 B. S. Prall, D. Y. Parkinson, N. Ishikawa and G. R. Fleming, *J. Phys. Chem. A*, 2005, **109**, 10870–10879.
6 A. J. Van Tassle, M. A. Prantil and G. R. Fleming, *J. Phys. Chem. B*, 2006, **110**, 18989–18995.
7 F. E. Doany, B. I. Greene and R. M. Hochstrasser, *Chem. Phys. Lett.*, 1980, **75**, 206–208.
8 R. J. Sension, A. Z. Szarka and R. M. Hochstrasser, *J. Chem. Phys.*, 1992, **97**, 5239–5242.
9 J. Y. Liu, W. H. Fan, K. L. Han, D. L. Xu and N. Q. Lou, *J. Phys. Chem. A*, 2003, **107**, 1914–1917.
10 T. Kasajima, S. Akimoto, S. Sato and I. Yamazaki, *J. Phys. Chem. A*, 2004, **108**, 3268–3275.
11 A. Pigliucci, G. Duvanel, L. M. L. Daku and E. Vauthey, *J. Phys. Chem. A*, 2007, **111**, 6135–6145.
12 T. Förster and K. Kasper, *Z. Phys. Chem., Neue Folge*, 1954, **1**, 275.
13 H. Staerk, W. Kuhnle, R. Treichel and A. Weller, *Chem. Phys. Lett.*, 1985, **118**, 19–24.
14 F. Lopez-Arbeloa, M. Van Der Auweraer, F. Ruttens and F. C. De Schryver, *J. Photochem. Photobiol., A*, 1988, **44**, 63–83.
15 L. Margulis, P. F. Pluzhikov, B. Mao, V. A. Kuzmin, Y. J. Chang, T. W. Scott and N. E. Geacintov, *Chem. Phys. Lett.*, 1991, **187**, 597–603.
16 U. Werner, A. Wiessner, W. Kuhnle and H. Staerk, *J. Photochem. Photobiol., A*, 1995, **85**, 77–83.
17 N. Ohta, T. Kanada, I. Yamazaki and M. Itoh, *Chem. Phys. Lett.*, 1998, **292**, 535–541.
18 R. De, Y. Fujiwara, T. Haino and Y. Tanimoto, *Chem. Phys. Lett.*, 1999, **315**, 383–389.
19 K. Wynne, G. D. Reid and R. M. Hochstrasser, *J. Chem. Phys.*, 1996, **105**, 2287–2297.
20 D. von Seggern, C. Modrakowski, C. Spitz, A. D. Schluter and R. Menzel, *Chem. Phys.*, 2004, **302**, 193–202.
21 S. T. Gaballah, Y. H. A. Hussein, N. Anderson, T. Q. T. Lian and T. L. Netzel, *J. Phys. Chem. A*, 2005, **109**, 10832–10845.
22 F. D. Lewis, P. Daublain, G. B. Delos Santos, W. Z. Liu, A. M. Asatryan, S. A. Markarian, T. Fiebig, M. Raytchev and Q. A. Wang, *J. Am. Chem. Soc.*, 2006, **128**, 4792–4801.
23 B. K. Kaletas, R. Dobrawa, A. Sautter, F. Wurthner, M. Zimine, L. De Cola and R. M. Williams, *J. Phys. Chem. A*, 2004, **108**, 1900–1909.
24 A. S. D. Sandanayaka, Y. Araki, O. Ito, G. R. Deviprasad, P. M. Smith, L. M. Rogers, M. E. Zandler and F. D'Souza, *Chem. Phys.*, 2006, **325**, 452–460.
25 J. Shirdel, A. Penzkofer, Z. Shen, R. Prochazka and J. Daub, *Chem. Phys.*, 2007, **337**, 99–109.
26 J. S. Kim and D. T. Quang, *Chem. Rev.*, 2007, **107**, 3780–3799.
27 M. Nepraš, O. Machalicky, M. Šeps, R. Hrdina, P. Kapusta and V. Fidler, *Dyes Pigm.*, 1997, **35**, 31–44.
28 S. Speiser, *Chem. Rev.*, 1996, **96**, 1953–1976.
29 S. Speiser and F. Schael, *J. Mol. Liq.*, 2000, **86**, 25–35.
30 V. Fidler, P. Kapusta, M. Nepraš, J. Schroeder, I. V. Rubtsov and K. Yoshihara, *Collect. Czech. Chem. Commun.*, 1998, **63**, 1460.
31 V. Fidler, P. Kapusta, M. Nepraš, J. Schroeder, I. V. Rubtsov and K. Yoshihara, *Z. Phys. Chem.*, 2002, **216**, 589–603.
32 C. Grimm, M. Kling, J. Schroeder, J. Troe and J. Zerbs, *Isr. J. Chem.*, 2003, **43**, 305–317.
33 M. Kopczynski, T. Lenzer, K. Oum, J. Seehusen, M. T. Seidel and V. G. Ushakov, *Phys. Chem. Chem. Phys.*, 2005, **7**, 2793–2803.
34 M. Nepraš *et al.*, unpublished work.
35 C. Heidelbach, V. Vikhrenko, D. Schwarzer and J. Schroeder, *J. Chem. Phys.*, 1999, **110**, 5286.
36 D. Schwarzer, J. Troe, M. Votsmeier and M. Zerezke, *J. Chem. Phys.*, 1996, **105**, 3121–3131.
37 M. L. Horng, J. A. Gardecki, A. Papazyan and M. Maroncelli, *J. Phys. Chem.*, 1995, **99**, 17311–17337.
38 Quantum chemical calculations were performed using the ORCA program package: F. Neese, University of Bonn, 2007; F. Neese, *J. Am. Chem. Soc.*, 2006, **128**, 10213; F. Neese, *J. Comput. Chem.*, 2003, **24**, 1740. Our DFT-calculations employed the BP86 functional (A. D. Becke, *Phys. Rev. A*, 1988, **38**, 3098; J. P. Perdew, *Phys. Rev. B*, 1986, **33**, 8822) and the Ahlrichs TZV(p,2d) basis using polarization functions from the TurboMole library: A. Schaefer, H. Horn and R. Ahlrichs, *J. Chem. Phys.*, 1992, **97**, 2571; K. Eichkorn, O. Treutler, H. Ohm, M. Haser and R. Ahlrichs, *Chem. Phys. Lett.*, 1995, **240**, 283; invoking the resolution of identity (RI) approximation: F. Neese, *J. Comput. Chem.*, 2003, **24**, 1740. Excited state energies were calculated employing the TD-DFT module of the ORCA-package.

This journal is © the Owner Societies 2009

Phys. Chem. Chem. Phys., 2009, **11**, 317–323 | 323